

## 4.0 BACKGROUND

Asbestos is a term used to describe the fibrous habit of a family of hydrated metal silicate minerals. The most widely accepted definition of asbestos includes the fibrous habits of six of these minerals (IARC 1977). The most common type of asbestos is chrysotile, which is the fibrous habit of the mineral serpentine. The other five asbestos minerals are all amphiboles (i.e. all partially hydrolyzed, magnesium silicates). These are: fibrous reibeckite (crocidolite), fibrous grunerite (amosite), anthophyllite asbestos, tremolite asbestos, and actinolite asbestos.

All six of the minerals whose fibrous habits are termed asbestos occur most commonly in non-fibrous, massive habits. While unique names have been assigned to the asbestiform varieties of three of the six minerals (noted parenthetically above) to distinguish them from their massive forms, such nomenclature has not been developed for anthophyllite, tremolite, or actinolite. Therefore, when discussing these latter three minerals, it is important to specify whether a massive habit of the mineral or the fibrous (asbestiform) habit is intended.

Although other minerals may also occur in a fibrous habit, they are not generally included in the definition of asbestos either because they do not exhibit properties typically ascribed to asbestos (e.g. high tensile strength, the ability to be woven, heat stability, and resistance to attack by acid or alkali) or because they do not occur in sufficient quantities to be exploited commercially.

The first four of the six asbestos minerals listed above have been exploited commercially (IARC 1977). Of these, chrysotile alone accounts for more than 90% of the asbestos found in commercial products.

Importantly, it is neither clear whether the term asbestos maps reasonably onto the range of fibrous minerals that can contribute to asbestos-like health effects nor whether individual structures of the requisite mineralogy must formally be asbestiform to contribute to such health effects.

Regarding whether the term asbestos is a useful discriminator for health effects, it is well established that erionite (a fibrous zeolite not related to asbestos) is a potent inducer of mesothelioma (Baris et al. 1987), which is one of the two primary asbestos-induced cancers (see Chapter 3). It is therefore possible that the fibrous habits of at least some other minerals not formally included in the current definition of asbestos may contribute to the induction of asbestos-related diseases. Therefore, what needs to be developed, is an efficient procedure for separating potentially hazardous materials from those that are most likely benign.

There are two issues related to the question of whether fibers must formally be asbestiform to contribute to health effects. The first involves the relationship between fiber structure and disease induction and the second involves measurement. Although the evidence is overwhelming that the size and shape of a fiber affects the degree to which it contributes to the induction of disease (see Chapter 7 and, specifically, Section 7.5), it does not appear that sizes inducing biological activity are well distinguished by criteria that define the asbestiform habit. For example, determining the concentration of a specific, common size range of structures was shown to adequately predict the observed tumorigenicity of six forms of tremolite (three asbestiform varieties and three non-asbestiform varieties) that were intrapleurally injected into rats (see Section Appendix B). Once again, therefore, what is needed is an efficient procedure for distinguishing between the potentially hazardous size range of fibrous structures and those that do not contribute to disease.

Importantly, depending on the definition employed for the fibers (or fibrous structures) that are counted during an analysis, it may or may not be necessary to distinguish formally between asbestiform and non-asbestiform structures for the concentrations derived from such a count to adequately reflect biological activity.

Note, the dimensions of an asbestiform fiber are determined by the manner in which the fiber grows (Addison, J. private communication). In contrast, the massive forms of various minerals, when cleaved, also form elongated particles (termed “cleavage fragments”) and, depending on the definition employed for fibrous structures during an analysis, such cleavage fragments may or may not be included along with asbestiform fibers in a count (see, Section 4.3). Although it is clear from the manner in which they are each formed that the surface properties of asbestiform fibers and cleavage fragments are likely to be very different (for example, the latter will have many “unsatisfied” chemical bonds), the degree to which such differences affect potency for comparable sized structures is not currently known.

Although it is beyond the scope of this document to present a detailed treatise on asbestos mineralogy, the morphology of asbestos dusts, or the nature and limitations of analytical techniques and methods used to determine asbestos concentrations, a brief overview of these topics is presented in the following sections both to identify issues that need to be addressed as part of the development of an appropriate protocol for assessing asbestos risks and to provide the background required to facilitate evaluation of the relevant issues. In that regard, a section on lung physiology and function is also provided.

## 4.1 THE MINERALOGY OF ASBESTOS

As previously indicated, the six asbestos minerals can be divided into two general classes.

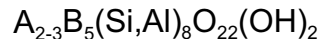
Chrysotile is the fibrous habit of the mineral serpentine (Hodgson 1965). The smallest fibrils of chrysotile occur as rolled sheets or hollow tubules of this magnesium silicate mineral. The larger fibers of chrysotile form as tightly packed bundles of the unit fibrils.

Chrysotile fibrils typically range from 20 nm to approximately 300 or 400 nm (0.02 to 0.3 or 0.4  $\mu\text{m}$ ) in diameter. Occasionally, structures up to 1000 nm (1  $\mu\text{m}$ ) have been observed, but these are unusual. At some point the curvature induced by the mismatch between the magnesium and silicon layers of the fibril becomes thermodynamically unstable, so that production of thicker fibrils is prohibited (Addison, J. private communication).

Chrysotile bundles are held together primarily by Van der Waals forces and will readily disaggregate in aqueous solutions containing wetting agents (e.g. soap). They will also readily disaggregate in lung surfactant (Addison, J. private communication).

The general chemical composition of serpentine is reported as  $\text{Mg}_3(\text{Si}_2\text{O}_5)(\text{OH})_4$  (Hodgson 1965). However, the exact composition in any particular sample may vary somewhat from the general composition. For example, aluminum may occasionally replace silicon and iron, nickel, manganese, zinc or cobalt may occasionally replace magnesium in the crystal lattice of chrysotile (serpentine).

The five other common varieties of asbestos are all fibrous forms of amphibole minerals (Hodgson 1965). These are ferro-magnesium silicates of the general composition:



where:

A = Mg, Fe, Ca, Na, or K; and

B = Mg, Fe, or Al.

Some of these elements may also be partially substituted by Mn, Cr, Li, Pb, Ti, or Zn.

The fibrous habits of the amphibole minerals tend to occur as extended chains of silica tetrahedra that are interconnected by bands of cations (Hodgson 1965). Each unit cell typically contains eight silica tetrahedra and the resulting fibers tend to be rhomboid in cross-section. Amphibole fibrils are generally thicker than chrysotile fibrils and may typically range from approximately 100 nm to 700 or 800 nm in diameter (Addison, J. private communication). Substantially thicker fibrils have also been observed.

## 4.2 MORPHOLOGY OF ASBESTOS DUSTS

Structures comprising the fibrous habits of the asbestos minerals come in a variety of shapes and sizes. Not only do single, isolated fibers vary in length and thickness but such fibers may be found combined with other fibers to form bundles (aggregates of closely packed fibers arranged in parallel) or clusters (aggregates of randomly oriented fibers) or combined with equant particles to form matrices (asbestos fibers embedded in non-asbestos materials). Consequently, dusts (even of one mineral variety) are complex mixtures of structures. For precise definitions of the types of fibrous structures typically found in asbestos dusts, see Chatfield and Berman (1990).

Detailed descriptions of the characteristics of dusts typically encountered at environmental and occupational asbestos sites have been reported in the literature and the following summary is based on a previously published review (Berman and Chatfield 1990). Typically, the major components of the dust observed in most environments are non-fibrous, isometric particles. Fibrous structures consistently represent only a minor fraction of total dust. Asbestos structures represent a subset of the fibrous structures.

The magnitude of the fraction of total dust represented by fibers and the fraction of fibers composed of asbestos minerals vary from site to site. However, the fraction of asbestos in total dusts has been quantified only in a very limited number of occupational and environmental settings (see, for example, Lynch et al 1970 or Cherrie et al 1987).

The gross features of structure size distributions appear to be similar among asbestos dusts characterized to date (Berman and Chatfield 1990). The major asbestos fraction of all such dusts are small structures less than 5  $\mu\text{m}$  in length. Length distributions generally exhibit a mode (maximum) between 0.8 and 1.5  $\mu\text{m}$  with larger fibers occurring with decreasing frequency. Fibrous structures longer than 5  $\mu\text{m}$  constitute no more than approximately 25% of total asbestos structures in any particular dust and generally constitute less than 10%.

In some environments, the diameters of asbestos fibers exhibit a narrow distribution that is largely independent of length. In other environments, diameters appear to exhibit a narrow distribution about a mean for each specific length. In the latter case, both the mean and the spread of the diameter distribution increases as the length of the structures increase. The increase in diameter with length appears to be more pronounced for chrysotile than for the amphiboles, presumably due to an increase in the fraction of chrysotile bundles contributing to the overall distribution as length increases.

Only a few studies have been published that indicate the number of complex structures in asbestos size distributions. The limited data available indicate that complex structures may constitute a substantial fraction (up to one third) of total structures, at least for chrysotile dusts (see, for example, Sebastien et al 1984). Similar results were also obtained during a re-analysis of dusts generated from the asbestos samples evaluated in the animal inhalation studies conducted by Davis et al. (Berman et al. unpublished). This is the same re-analysis used to support a study to identify asbestos characteristics that promote biological activity (Berman et al. 1995), which is discussed further in Section 7.4.3.

Historically, fibrous structures have been arbitrarily defined as structures exhibiting aspect ratios (the ratio of length to width) greater than 3:1 to distinguish them from isometric particles (Walton, 1982). However, alternate definitions for fibers have also been proposed, which are believed to better relate to biological activity (see, for example, Wylie et al. 1993 or Berman et al. 1995). The degree to which fibers are combined within complex structures in a particular dust may also affect the biological activity of the dust (Berman et al. 1995). Therefore, proper characterization of asbestos exposure requires that the relative contributions from each of many components of exposure be simultaneously considered. Factors that need to be addressed include the distribution of structure sizes, shapes, and mineralogy in addition to the absolute concentration of structures. Such considerations are addressed further in Chapter 7. Thus, unlike the majority of other chemicals frequently monitored at hazardous wastes sites, asbestos exposures cannot be adequately characterized by a single concentration parameter.

#### **4.3 CAPABILITIES OF ANALYTICAL TECHNIQUES USED TO MONITOR ASBESTOS**

Due to a complex history, a range of analytical techniques and methods have been employed to measure asbestos in the various studies conducted over time (Walton 1982). Use of these various methods has affected the comparability of results across the relevant asbestos studies (Berman and Chatfield 1990). Therefore, the relative capabilities and limitations of the most important methods used to measure asbestos are summarized here. Later sections of this report incorporate attempts to reconcile effects that are attributable to the limitations of the different methods employed in the various studies evaluated.

Analytical techniques used to measure airborne asbestos concentrations vary greatly in their ability to fully characterize asbestos exposure. The capabilities and limitations of four analytical techniques (midget impinger, phase contrast microscopy, scanning electron microscopy, and transmission electron microscopy) need to be considered here.

Midget impinger (MI) and phase contrast microscopy (PCM) are the two analytical techniques used to derive exposure estimates in the majority of epidemiology studies from which the existing risk factors are derived. Scanning electron microscopy (SEM) is an analytical technique that has been employed in several key animal studies. Transmission electron microscopy (TEM) provokes interest because it is the only analytical technique that is potentially capable of distinguishing all of the characteristics of asbestos that potentially affect biological activity.

Although PCM is widely used to characterize occupational exposures, its inability to distinguish between asbestos and non-asbestos and its lack of sensitivity limits its usefulness in environmental settings (Berman and Chatfield 1990). In fact, PCM analyses and TEM analyses showed no correlation among measurements collected during the cleanup of the Oakland Hills fire (Berman, unpublished). Such lack of correlation is expected to be observed generally whenever measurements are collected at sites where no single, obvious source of asbestos is expected to dominate. Consequently, TEM is the technique that has been recommended for use at Superfund sites (Chatfield and Berman 1990 and Berman and Kolk 1997).

A general comparison of the relative capabilities and limitations of the analytical techniques introduced above is presented in Table 4-1.

Importantly, the physical limitations of the various analytical techniques is only part of the problem. To provide reproducible results that can be compared meaningfully to other analyses in other studies, one must also consider the choice of procedures (methods) that address everything from sample collection and preparation to rules for counting and quantifying asbestos structures.

Multiple methods have been published for use in conjunction with several of the analytical techniques mentioned above (particularly TEM). Such methods differ in the procedures incorporated for sample preparation and for the manner in which asbestos structures are counted. The sample preparation requirements, conditions of analysis, and structure counting rules for several of the most commonly employed methods are presented in Table 4-2 to illustrate how the choice of method can result in substantially different measurements (even on duplicate or split samples).

**Table 4-1:**  
**Capabilities and Limitations of Analytical Techniques Used for**  
**Asbestos Measurements<sup>1</sup>**

Parameter	Midget Impinger	Phase Contrast Microscopy	Scanning Electron Microscopy	Transmission Electron Microscopy
Range of Magnification	100	400	2,000 - 10,000	5,000 - 20,000
Particles Counted	All	Fibrous Structures <sup>2</sup>	Fibrous Structures <sup>2</sup>	Fibrous Structures <sup>2,3</sup>
Minimum Diameter (size) Visible	1 µm	0.3 µm	0.1 µm	< 0.01 µm
Resolve Internal Structure	No	No	Maybe	Yes
Distinguish Mineralogy <sup>4</sup>	No	No	Yes	Yes

1. The capabilities and limitations in this table are based primarily on the physical constraints of the indicated instrumentation. Differences attributable to the associated procedures and practices of methods in common use over the last 25 years are highlighted in Table 4-2.
2. Fibrous structures are defined here as particles exhibiting aspect ratios (the ratio of length to width) greater than 3 (see Walton 1982).
3. TEM counts frequently resolve individual fibrous structures within larger, complex structures. Based on internal structure, several different counting rules have been developed for handling complex structures. See the discussion of methods presented below.
4. Most SEM and TEM instruments are equipped with the capability to record selected area electron diffraction (SAED) spectra and perform energy dispersive X-ray analysis (EDXA), which are used to distinguish the mineralogy of structures observed.

The second column of Table 4-2 describes the specifications of the PCM method currently mandated by the Occupational Safety and Health Agency (OSHA) for characterizing asbestos exposure in occupational settings. Although this method is in common use today, several alternate methods for counting fibrous structures by PCM

TABLE 4-2, Page 1



Table 4-2, Page 2

Table 4-2, Page 3

have also been used historically. Therefore, PCM measurements reported in earlier studies (including the available epidemiology studies) may not be comparable to PCM results collected today.

The last four columns of Table 4-2 describe TEM methods that are in current use. Comparison across these methods indicates:

- the shortest lengths included in counts using these methods vary between 0.06 and 1  $\mu\text{m}$ . Given that structures shorter than 1  $\mu\text{m}$  represent a substantial fraction of total asbestos structures in almost any environment (Section 4.2), this difference alone contributes substantially to variation in measurement results across methods;
- the definitions and procedures for counting complex structures (i.e. bundles, clusters, and matrices) vary substantially across methods, which further contribute to variation in measurement results. For example, the ISO Method requires that component fibers of clusters and matrices be counted separately, if they can be readily distinguished. In contrast, clusters are counted as single structures under the AHERA Method; and
- although all of the methods listed incorporate sample preparation by a direct transfer process, several of the methods have also been paired with an optional indirect transfer process. Measurements derived from split samples that are prepared, respectively, by direct and indirect transfer, can vary by factors as large as several 100 (Berman and Chatfield 1990). More typically, however, counts of asbestos structures on samples prepared by an indirect transfer procedure are greater than those derived from directly prepared samples by factors of between 5 and 50.

Given the combined effects from the physical limitations of the various techniques employed to analyze for asbestos and the varying attributes of the methods developed to guide use of these techniques, the relative capabilities and limitations of asbestos measurements derived, respectively, from paired methods and techniques in common use can be summarized as follows:

- all four techniques are particle counting techniques;
- neither MI nor PCM are capable of distinguishing asbestos from non-asbestos (i.e. they are incapable of determining structure mineralogy);
- counting rules used in conjunction with MI do not distinguish isometric particles from fibers;

- counting rules used in conjunction with PCM limits counting to fibrous structures longer than 5  $\mu\text{m}$  with aspect ratios greater than 3:1;
- the range of visibility associated with PCM limits counting to fibers thicker than approximately 0.3  $\mu\text{m}$ ;
- under conditions typically employed for asbestos analysis, the range of visibility associated with SEM limits counting to fibers thicker than approximately 0.1  $\mu\text{m}$ , which is only marginally better than PCM;
- SEM is capable of distinguishing asbestos structures from non-asbestos structures;
- TEM is capable of resolving asbestos structures over their entire size range (down to thicknesses of 0.01  $\mu\text{m}$ );
- TEM is capable of distinguishing the internal components of complex asbestos structures; and
- TEM is capable of distinguishing asbestos structures from non-asbestos structures.

More detailed treatments of the similarities and differences between asbestos techniques and methods can also be found in the literature (see, for example, Berman and Chatfield 1990).

Due to the differences indicated, measurements from a particular environment (even from duplicate samples) that are derived using different analytical techniques and methods can vary substantially and are not comparable. In fact, results can differ by two or three orders of magnitude (Berman and Chatfield 1990). More importantly, because the relative distributions of structure sizes and shapes vary from environment to environment, measurements derived using different analytical techniques and methods do not even remain proportional from one environment to the next. Therefore, the results from multiple asbestos studies can only be meaningfully compared if the effects that are attributable to use of differing analytical techniques and methods can be quantified and reconciled. To complicate the situation, however, few of the existing studies document analytical procedures in sufficient detail to reconstruct exactly what was done.

## 4.4 THE STRUCTURE AND FUNCTION OF THE HUMAN LUNG

### 4.4.1 Lung Structure

The lungs are the organs of the body in which gas exchange occurs to replenish the supply of oxygen and eliminate carbon dioxide. To reach the gas exchange regions of the lung, inhaled air (and any associated toxins) must first traverse the proximal conducting (non-respiratory) airways of the body and the lung including the nose (or mouth), pharynx, larynx, trachea, and the various branching bronchi of the lungs down to the smallest (non-respiratory) bronchioles. Air then enters the distal (respiratory) portion of the lung, where gas exchange occurs.

In humans, the respiratory portion of the lungs are composed of the respiratory or aveolarized bronchioles, the alveolar ducts, and the alveoli (or alveolar sacs). There are approximately  $3 \times 10^8$  alveoli in human lungs (about 20 per alveolar duct) with a cumulative volume of  $3.9 \times 10^3 \text{ cm}^3$  (Yeh and Harkema 1993). This represents approximately 65% of the total volume capacity of human lungs at full inspiration.

Yeh and Harkema also report that the ratio of lung volume to body weight is approximately constant across a broad range of mammals (from a shrew - 0.007 kg to a horse - 500 kg). Human lung volumes average a little more than 5 L.

Each human alveolus has a diameter of approximately 0.03 cm (300  $\mu\text{m}$ ) and a length of 0.025 cm (Yeh and Harkema 1993). The typical path length from the trachea to an alveolus is approximately 25 cm. The bronchi leading to each alveolus have branched an average of 16 times from the trachea (with a range of 9 to 22 branches). Importantly, the mean path length, the number of branches between trachea and alveolus, and the detailed architecture (branching pattern) of the respiratory region of the lung vary across mammalian species. For example, rats and mice lack respiratory bronchioles while macaque monkeys exhibit similar numbers of respiratory bronchiole generations as humans (Nikula et al. 1997). Furthermore, branching in humans tends to be symmetric (each daughter branch being approximately the same size and the angle of branching for each is similar but not quite equal) while rodents tend to exhibit monopodal branching in which smaller branches tend to come off at angles from a main trunk (Lippmann and Schlesinger 1984).

The gas exchange regions of the lung are contained within the lung parenchyma, which constitute approximately 82% of the total volume of the lungs (Gehr et al. 1993). Importantly, the lung parenchyma is not a “portion” of the lung; it fills virtually the entire volume of the organ traditionally visualized as the “whole” lung. Embedded within the parenchyma are the larger conducting airways of the lungs and the conducting blood vessels that transport blood to and from the capillaries that are associated with each alveolus. In the human lung, approximately 213 ml of blood are distributed over  $143 \text{ m}^2$

of gas-exchange (alveolar) surface area (about the size of a tennis court). The gas-exchange surface area of lungs scale linearly with body weight over most mammalian species. The slope of the line is 0.95. Figure 4-1 is a photomicrograph showing two views of a portion of lung parenchyma in the vicinity of a terminal bronchiole and an alveolar duct, which are labeled. The circular spaces in the left portion of the figure and the cavities in the right portion of the figure are alveoli. Note the thinness of the walls (septa) separating alveoli.

Alveoli are separated from each other by alveolar septa that average only a few micrometers in thickness (Gehr et al. 1993). Gas-exchange capillaries run within these septa and the air-blood barrier, which averages only 0.62  $\mu\text{m}$  in thickness, is composed of three layers: the alveolar epithelium, the interstitium, and endothelium. The epithelium is described in detail below. The interstitium is primarily composed of a collagenous, extracellular matrix, which constitute about two-thirds of the volume with a collection of fibroblasts, macrophages, and other cells interspersed within the matrix (Miller et al. 1993). The cells of the interstitium constitute about one third of its volume. The endothelial layer is composed of the smooth muscle cells and connective tissue that constitute the walls of vascular capillaries. The amount of connective tissue in the septa between alveoli also varies between animal species; small rodents have less and primates more (Nikula et al. 1997).

Figures 4-2 and 4-3 show, respectively, a typical alveolar septum and a closeup of one portion of such a septum. In Figure 4-2, one can see that the septa themselves are thin and are filled almost entirely with capillaries. Figure 4-3 shows that the epithelial lining of an alveolus is no more than 1  $\mu\text{m}$  thick, that the underlying interstitium is no thicker, and that the endothelium of the adjacent capillary is similarly thin. These three layers constitute the major tissues of the air-blood barrier (the rest of the barrier includes the limited quantity of blood plasma between the endothelial wall of a capillary and a red blood cell and the outer membrane of the red blood cell itself).

Gehr et al. (1993) also report that interalveolar septa constitute approximately 14% of the volume of the gas-exchange region of the lung (i.e. the lung parenchyma). Of this tissue mass, approximately 20% is endothelium, 55% is interstitium, and the rest is composed of cells associated with the alveolar epithelium. The remainder of the gas-exchange region is air space. Gehr et al. also report that the interalveolar septa fold to accommodate changes in lung volume during respiration, although the major contribution to lung volume changes (over the range of normal inspiration) appears to be the collapsing (folding) of alveolar ducts (Mercer and Crapo 1993).

Figure 4-1

Figure 4-2



Figure 4-3

According to Gehr et al. (1993), human alveoli contain approximately 380 cells and the total number reportedly increases as a power function with body mass for other mammals. In humans, this includes approximately 12 alveolar macrophages (although this number is larger in smokers, apparently due to chronic inflammation), 40 Type I epithelial cells, 67 Type II epithelial cells, 106 interstitial cells, and 148 endothelial cells.

The relative number of the various types of cells associated with alveoli varies across mammalian species (Gehr et al. 1993). In the rat, for example, Type I epithelium is approximately 20% of the total (rather than 12% in humans) with less interstitium and more endothelium.

According to Gehr et al. (1993), Type I epithelial cells, which constitute approximately 95% of the surface area of alveolar epithelium, are flat and platy (squamous), and average less than 1  $\mu\text{m}$  in thickness (except where cell nuclei exist, which are approximately 7.5  $\mu\text{m}$  in diameter and protrude into the alveolar space). Type II epithelial cells, which are cuboidal, constitute no more than 5% of the epithelial surface. Despite the small fraction of surface that they occupy, Type II cells serve to maintain the integrity of the overall epithelial lining so that, for example, they limit the tissue's permeability and control/prevent transport of macromolecules from the interstitium to the alveolar space, or the reverse (Leikauf and Driscoll 1993). Type II cells also secrete lung surfactant. The basement membrane of alveolar epithelium is a collagenous structure.

In contrast, the epithelial cells lining the trachea and bronchi (including the respiratory bronchioles) are ciliated and columnar and averages between 10 and 15  $\mu\text{m}$  in thickness (based on photomicrographs presented in St. George et al. 1993). Tracheobronchial epithelium reportedly contains at least 8 distinct cell types (St. George et al. 1993): ciliated epithelium, basal cells (small flat cells situated along the basal lamina and not reaching the luminal surface), mucous goblet cells, serous cells, nonciliated bronchiolar (clara) cells, small mucous granule (SMG) cells, brush cells, and neuroendocrine cells. The relative abundance of the various cells varies across mammalian species as well as across the various airway generations (branches) and even the opposing sides of specific airways. The number of cells per length of basal lamina also varies across mammalian species.

#### 4.4.2 The Structure of the Mesothelium

The mesothelium is a double layered membrane and each layer is a single-cell thick. The two layers of the mesothelium are separated by a space (e.g. the pleural space), which contains extracellular fluid and free macrophages (Kane and McDonald 1993). The pleural space is drained at fixed locations by lymphatic ducts. Each layer of the mesothelium overlies a collagenous basement membrane containing dispersed spindle cells. Depending on the location of the mesothelium, the basement membrane may

overlie the skeletal muscle of the diaphragm or the rib cage (in the case of the parietal pleura, which is the outer layer). For the inner layer or visceral pleura, the basement membrane overlies visceral organs (including the lungs) within the rib cage. Healthy mesothelium is quiescent, meaning that cells are not actively dividing.

The relative size and thickness of mesothelial tissue varies across mammalian species (Nikula et al. 1997). For example, rats have relatively thin pleura with limited lymphatic ducts. In contrast, nonhuman primates have thicker pleura with greater lymphatic drainage than rats and humans have even thicker pleura and relatively abundant lymphatic ducts.

#### 4.4.3 Cytology

**Alveolar Epithelium.** In the respiratory region of the lung, Type II epithelial cells are progenitor cells for Type I epithelium (Leikauf and Driscoll 1993). Type I epithelial cells are not proliferation competent (Nehls et al. 1997). After injury to Type I cells, Type II cells proliferate and reestablish the continuous epithelial surface. Type II cells also secrete surfactant. It appears that the identity and location of the progenitor cells for Type II epithelial cells are not currently known.

Injury or alteration of Type II cell function are associated with several diseases included idiopathic pulmonary fibrosis (Leikauf and Driscoll 1993). Also, crystalline silica and other toxic agents have been shown to directly modify Type II cellular activity. For example, crystalline silica (at sub-cytotoxic levels, < 100 µg/ml) stimulates Type II proliferation in tissue culture. In contrast, neither titanium dioxide nor aluminum coated silica induce proliferation at corresponding concentrations.

In culture, Type II epithelial cells transform slowly into Type I cells and thus have limited population doubling capacity (Leikauf and Driscoll 1993). Rarely can the number of Type II cells expand past three to 10 passages (20-30 doublings). During this time, cells terminally differentiate, develop cross-linked envelopes, and appear squamous, enlarged, and multinucleated. The process is noted to be accelerated by the presence of transforming growth factor beta (TGF-β).

**Macrophages.** Alveolar macrophages (the largest population of macrophages in the lung) are mobile, avidly phagocytic, present antigens, and release cytokines that trigger various other immune responses (Leikauf and Driscoll 1993). They also initiate inflammatory responses and other repair mechanisms that are designed to restore tissue homeostasis.

The next largest population of macrophages in the lung are the interstitial macrophages (Leikauf and Driscoll 1993). These are localized in the peribronchial and perivascular spaces, the interstitial spaces of the lung parenchyma, the lymphatic channels, and the

visceral pleura. The various populations of macrophages in the lung express different surface proteins, show different proliferative capacity, and show differences in metabolism.

The sizes of alveolar macrophages varies substantially across mammalian species (Krombach et al. 1997). Krombach and co-workers provide a table summary of the relative sizes across several species of interest:

Animal	Mean diameter (um)	Mean Volume (um <sup>3</sup> )
Rats	13.1 +/-0.2	1166 +/-42
Syrian Golden Hamsters	13.6 +/-0.4	1328 +/-123
Cynomolgus Monkeys	15.3 +/-0.5	
Healthy Humans	21.2 +/-0.3	4990 +/-174

As indicated later (Section 7.2), the relative size of various macrophages has direct implications regarding the dependence of clearance mechanisms on fiber size.

**Mesothelium.** Importantly, mesothelial cells are proliferation competent and may be their own progenitor cells (Kane and McDonald 1993). It is also possible, however, that as yet to be identified progenitor cells are located along opposite walls of pleura or at other locations within the pleural space.

**Tracheo-bronchiolar epithelium.** As previously indicated, tracheo-bronchiolar (i.e. non-respiratory) epithelium is composed primarily of ciliated, columnar cells that are 10 to 15 µm thick. Although some report that Clara cells serve as progenitor cells for tracheo-bronchiolar epithelium (Finkelstein et al. 1997), others report that both Clara cells and bronchiolar epithelium are proliferation competent (Nehls et al. 1997). It appears that the identity and location of the progenitor cells for Clara cells are not currently known.

#### 4.4.4 Implications

The potential implications of the above observations concerning lung structure and cytology are:

- that the thicknesses of Type I epithelial cells, endothelial cells, and the interstitium in the alveolar septa are all very small relative to the lengths of the putative asbestos fibers that contribute to disease;
- that an entire alveolus is only 300 µm across and a typical Type I cell is 46 µm in radius by < 1 µm thick;

**PRELIMINARY WORKING DRAFT – DO NOT COPY OR QUOTE**

- that distances across alveolar septa are only on the order of a few  $\mu\text{m}$  and such septa contain both the endothelium and the interstitium. Thus, the distances that have to be traversed to get to these structures are also small relative even to the length of a fiber;
- that the alveolar septa and the walls of the alveolar ducts fold during respiration, which may provide mechanical forces that facilitate movement of fibers into and through the alveolar epithelium;
- that Type I epithelium do not proliferate so they cannot be the cells that lead to cancer. It is the Type II epithelial cells (and potentially macrophages, basal cells, or endothelial cells) that contribute to cancer in the pulmonary portion of the lung. Type II cells eventually terminally differentiate to Type I cells;
- that other cells in the lung that have variously been reported to be proliferation competent (so that they potentially serve as target cells for the induction of cancer) include Clara cells and bronchiolar epithelial cells;
- that the distance from the most distal airways and alveoli to the pleura is small relative to the lengths of a fiber; and
- that mesothelial cells are proliferation competent and thus serve as potential targets for the induction of cancer;